Observations and modeling of sea splash icing

Kathleen F. Jones and Keran J. Claffey
Cold Regions Research and Engineering Laboratory, Hanover, New Hampshire, U.S.A.
kathleen.f.jones@usace.army.mil

Abstract: Stationary offshore structures are subject to icing from sea spray and from run-up and splash. Sea spray is created by the bursting of bubbles in whitecaps and, at very high wind speeds, by water sheared from the crest of waves by the wind. The relatively large drops in this spindrift can result in significant ice accretion on any offshore structure in cold temperatures with wind speeds greater than about 20 m/s. For offshore structures with significant area at the waterline, waves running up on the side of the structure create large quantities of splash even at lower wind speeds. The relatively warm splash keeps ice from forming on the structure near the ocean surface even in subfreezing temperatures. The water content in the splash decreases with elevation and if the air is cold enough there may be sufficient cooling to freeze some or all of the water. In this paper we present observations of splash icing on a mast on Mt. Desert Rock in January-February 2014. We also develop a simple model of run-up and splash based on wave tank experiments and field observations. We compare the icing profile on the mast with model results using local observations of wind speed, air and water temperature, and significant wave height and period.

Keywords: icing, run-up, splash, off-shore structure

NOMENCLATURE

c_s	scatter coefficient= $\pi D/\lambda$
d	water depth (m)
D	diameter (width) of structure (m)
fr	splash fraction
g	acceleration of gravity (m/s^2)
H	wave height (m)
k	wave number= $2\pi/\lambda$ (m^{-1})
m	run-up and splash parameter
R	run-up height (m)
s_0	wave steepness = $2\pi H/gT^2$
S	splash height (m)
T	wave period (s)
u	water particle velocity at η_{max} (m/s)
U	wind speed (m/s)
W	liquid water content (g/m^3)
z	height above mean sea level (m)
η_{max}	height of wave crest (m)
ω	wave frequency= $2\pi/T$ (s^{-1})
λ	wave length (m)
π	3.14159
ρ_w	density of water
χ	tide height relative to mean sea level (m)

INTRODUCTION

Stationary offshore structures are subject to icing from sea spray and from run up and splash. Sea spray is created by the bursting of bubbles in whitecaps and, at very high wind speeds, by water sheared from the crest of waves by the wind. Icing may also occur as a result of wave interaction with a structure. For offshore structures with significant area at the waterline, waves running up on the side of the structure can create large quantities of splash even at wind speeds less than 20 m/s.

In this paper we present observations of icing on a mast at the water's edge on a small rocky island in the Gulf of Maine. Run-up and splash on the mast occurred as waves hit the near-vertical rock wall seaward of the mast. In the next section we present our observations of icing on Mt Desert Rock during the second Winter Rock Experiment (WREx2) in January-February 2014. In Section III we develop a model for run-up and splash icing on structures where that may be significant, namely those with significant area at the waterline. The model is based on observations of run-up and splash in wave tank experiments and at a breakwater. We relate splash and run-up height to the scatter coefficient, and suggest a simple variation for the splash liquid water content with height above the mean water surface. In Section IV we apply this model to measurements from WREx2.

I. BACKGROUND

Wave run-up on offshore structures is given as a function of the scatter coefficient $c_s = \pi D/\lambda$ in [1] based on observations in a wave tank of run-up on a partially submerged cylinder. The maximum run-up from mean sea level is given by

$$R_{\max} = 0.5H_{\max}\left(2.06 + 2.33c_s - 1.32c_s^2\right) + 0.5H_{\max}.$$

where H_{max} is the maximum wave height. Note that for c_s>0.9, the run-up height decreases as the ratio of structure width to wavelength increases. At the point of maximum wave force on the structure, which also depends on c_s, the numerical model N_RIGICE ejects droplets from the wave. The mass of water in the surface of each wave that is ejected as drops is specified by the code, but not described in [1] , and can be adjusted by a user-specified calibration parameter. N_RIGICE also includes a module for wind-generated spray, with a user-specified minimum wind speed for spray generation, using W from [2]. Small changes to these two user-specified parameters can drastically change the model results [1].

Forest et al [3] develop an equation for liquid water content in spray as a function of the significant wave height for their model RIGICE04. The liquid water content is based on measurements from the man-made Tarsuit Island, a drilling caisson structure with walls made of concrete boxes. They compare results from this model with N_RIGICE using weather data from the 2-year deployment of the Rowan-Gorilla III rig (Figure 1) near Sable Island, Nova Scotia. That rig has minimal area at the waterline so little tendency to generate run-up and splash. Based on the two models, they expected significant icing on the rig in more than a dozen weather events. However, the only event in which the icing sensors mounted on the rig showed any indication of ice accretion was also the only event with winds exceeding 20 m/s. This indicates that the source of the ice was probably sea spray generated over the open ocean, rather than splash from the interaction of the waves with the structure.

Kulyakhtin and Tsarau [4] use the Mitten [1] run-up equation but with a maximum run-up equal to the significant wave height H_s for $c_s \geq 0.9$. The sea spray flux in their icing model for fixed offshore structures depends on wind speed, wave period, significant wave height, and height above mean

sea level, but includes nothing to characterize the interaction of the structure with waves. Run-up is calculated only to determine the portion of the structure that is washed by waves and kept free of ice.

In this paper we follow Mitten [1], treating run-up and splash together—splash as a continuation of the run-up of green water on the structure—for structures with significant area at the waterline. Our model is simpler than N_RIGICE and has no user-specified parameters.

Figure 1: Rowan Gorilla III drill rig.

II. Observations

We observed splash icing on a mast near the water's edge on Mt. Desert Rock in the Gulf of Maine during the second Winter Rock Experiment (WREx2) in January and February 2014. The average salinity in this part of the Gulf of Maine was 33 psu. On days when the rock at the base of the mast was above the waves, we collected ice samples from the mast for salinity measurements. When the air temperature was below freezing, the surface of the accreted ice was hard and shiny with features that appeared to have been formed by rivulets of water flowing down and around toward the lee side of the mast under the influence of wind and gravity (Figure 2). Cleats, blocks, shackles, and ropes wrapped around the mast interrupted this water flow at about 0.5 m above the base. There was typically no ice below this level and many small icicles on the ropes and gear (Figure 3).

We collected small samples for salinity measurements by chipping ice from the accretion on the mast or by breaking off sometimes dripping icicles on 11 days between 23 Jan and 18 Feb. The ice in all of our 40 non-icicle samples was solid, with

Figure 2. Profile of splash icing on the mast on Mount Desert Rock, 17 Feb 2014.

Figure 3. Icicle formation on the ropes and gear on the mast on Mt. Desert Rock, 23 Jan 2014.

no entrapped water. The samples had a median salinity of 12 psu, with 25th and 75th percentile values of 10 and 19 psu. The icicle salinity was higher, with a median salinity of 29 psu for the 20 samples, and 25th and 75th percentile values of 21 and 33 psu. The highest icicle salinity was 65 psu.

Photographs of the mast taken almost every day from 22 Jan to 18 Feb shown in Figure 4 illustrate the evolution of the ice accretion on the mast from run-up and splash.

III. Run-up and splash model

The height of the run-up and the height of splash in our model are based on the formulation in De Vos et al [5], extended to encompass the wave tank observations of splash by Ramirez et al [6] and the observations of splash caused by wave interaction with a breakwater by Yamashiro et al [7].

De Vos et al [5] were interested in wave run-up on wind turbine foundations that could damage the platform and boat landing facilities that provide access to the turbine. They carried out small-scale wave tank tests and characterized the 2% run-up using a velocity head stagnation model with a parameter *m* that depends on the shape of the foundation and the steepness of the wave, with run-up decreasing with steepness:

$$R_{2\%} = \eta_{\max} + m\frac{u^2}{2g} \tag{1}$$

where u is the water particle velocity at the wave crest $\eta_{\max}$, both given by second order Stokes theory:

$$\eta_{\max} = \frac{H}{2} + k\frac{H}{2}\frac{H}{8}\frac{\cosh(kd)}{\sinh^3(kd)}\left(2+\cosh(2kd)\right)$$
$$u = \frac{Hgk}{2\omega}\frac{\cosh\left(k\left(\eta_{\max}+d\right)\right)}{\cosh(kd)} + \frac{3H^2k\omega}{16}\frac{\cosh\left(2k\left(\eta_{\max}+d\right)\right)}{\sinh^4(kd)} \tag{2a}$$

In deep water ($kd \to \infty$) these relationships can be simplified and provide lower bounds on u and $\eta_{\max}$:

$$\eta_{\max} = \frac{H}{2} + k\frac{H^2}{8}$$
$$u = \frac{Hgk}{2\omega}. \tag{2b}$$

To calculate $R_{2\%}$ in (1), the 2% wave height $H_{2\%}$, which can be estimated by $H_{2\%} = 1.4H_s$ is used in (2a) and (2b).

Ramirez et al [6] did the same kind of wave tank tests as [5] and used high-speed video to determine the run-up height of both green water and splash on slender piles. Keeping the

Figure 4. Icing on the mast on Mt. Desert Rock during WREx2.

formulation in terms of 2nd order Stokes theory for simplicity (rather than stream function theory used in [8] results in the following relationships between m and wave steepness s_0

$$m_g = -66.67 s_0 + 4.53 \text{ for } s_0 < 0.035$$
$$= 2.2 \qquad \text{for } s_0 > 0.035 \tag{3a}$$

for run-up R and

$$m_s = -200 s_0 + 13.6 \text{ for } s_0 < 0.035$$
$$= 6.6 \qquad \text{for } s_0 > 0.035 \tag{3b}$$

for splash S. While some offshore platforms have slender piles supporting the platform, others such as Molikpaq (Figure 5) have significant area at the waterline. To extend the formulation above to those sorts of structures, we used observations of splash generated by wave interaction with a vertical-sided breakwater. Yamashiro et al [7] used high-speed video to document the height of splash. The breakwater is 140 m wide with a top at 6.4 m above mean sea level. Splash from wave interaction with breakwater went as high as 57 m above the top of the breakwater with winds in the 9 to 12 m/s range and significant wave heights between 2 and 3 m. Using the splash height histograms in [7] along with histograms from the other observations (personal communication, Masaru Yamashiro) for the five periods when a) the breakwater had the original vertical sides, and b) the significant wave height and period are available, we calculated the 2% splash heights above mean sea level. In this calculation we assumed that the occurrence frequencies of splash at 2 and 4 m above the breakwater (which were not documented) were the same as the frequency at 6 m. Using the five cases from [7] and the three cases from [6],

Figure 5: Molikpaq drill rig.

shown in Table 1, we determined a relationship between m_s and c_s and between the fraction of time with splash *fr* and c_s:

$$m_s = 4.7 + 24.1c_s$$
$$fr = 0.055 + 0.0878c_s \le 0.78 \quad (4)$$

In our run-up and splash model, the m_s function of the c_s in (4) replaces the m_s function of s_0 in (3b). However there are no measurements of run-up on the breakwater to replace (3a). Run-up is limited by the height of the obstacle. If the calculated run-up from (3a) is greater than height of the obstacle, the splash height is decreased by the excess, as the waves interacting with the structure are not constrained to move vertically above the top of the structure.

Table 1. Splash data from [6] and [7]

D m	H_s m	c_s	s_0	*fr*	*S* m
0.56	1.05	0.072	0.033	0.026	1.57
0.56	1.1	0.052	0.02	0.032	2.22
0.56	1.1	0.058	0.02	0.080	3.52
140	1.66	8.34	0.04	0.617	25.4
140	2.2	6.75	0.036	0.648	41.4
140	2.33	6.49	0.04	0.706	31.4
140	1.78	7.62	0.038	0.767	33.4
140	1.78	7.3	0.04	0.782	26.4

To characterize the occurrence rate of various splash heights as a function of the 2% height, we combined all five breakwater cases to remove the effects of the variation in wind direction and the steadiness of the wind on the shape of the splash height distribution. This combined cumulative distribution of splash heights up to the 2% height is fit by

$$F = 1.01 - 1.197\exp\left(-0.118S_{\max}\right) \quad (5)$$

with a maximum splash height S_{max}=40 m.

What is the liquid water content in the splash plumes? We assume that there is green water at the significant wave height z=0.5H_s, so the liquid water content at that height above the current tide level is the density of water ρ_w. From that level the liquid water content decreases exponentially to W_s at the apparent top of the splash plume. This results in

$$W(z) = W_s\left(\frac{\rho_w}{W_s}\right)^{\frac{S-z}{S-0.5H_s}}. \quad (6)$$

with the plume extending above *S* with decreasing *W*(*z*). We take W_s=10 g/m^3, high enough for the splash above the breakwater to be visible at *S*.

For each time interval in the analysis, we calculate η_{max} and *u* from $H_{2\%}$, m_g from (3a), m_s from (4), and then $R_{2\%}$ and $S_{2\%}$ from (1). The splash plume liquid water content at height *z* is made up of superposed plumes with maximum heights above the tide level varying from 0.5H_s to $S_{2\%}$. The total splash in the time interval is the plume liquid water content multiplied by the fraction of time with splash from (4).

Examples of liquid water content profiles for the conditions in WREx2 are shown in Figure 6 for a 4-m wide obstacle (the approximate width of the rock face below the mast). The weather and ocean data and calculated splash parameters *S* and *fr* for these cases are in Table 2, in order of decreasing wind speed. Notice that the liquid water content in the plume depends on the dominant wave length and tide as well as on wind speed and significant wave height. For lower tides the impacting wave is carried higher above the obstacle as splash rather than flowing over it.

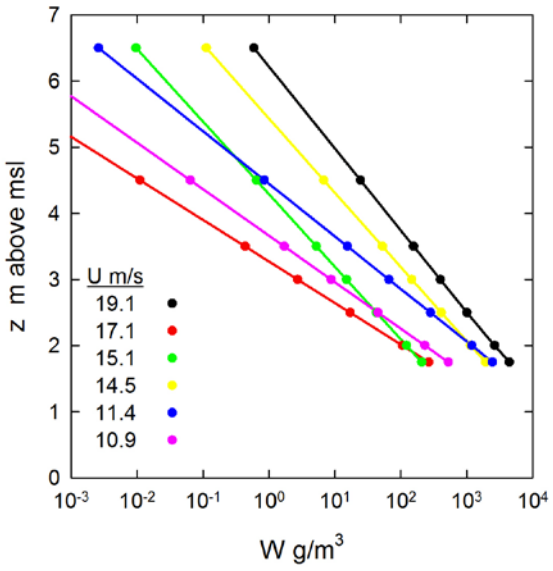

Figure 6. Examples of splash plume liquid water content from WREX2 weather and ocean data and a 4-m-wide rock face.

Table 2. Wind and ocean data and calculated splash parameters for the splash liquid water content profiles in Figure 6.

U m/s	H_s m	λ m	χ m	*fr*	*S* m
19.1	3.0	43.9	-0.5	0.08	7.7
17.1	3.0	64.0	-1.0	0.07	4.7
15.1	2.0	33.0	-1.4	0.09	6.4
14.5	1.9	25.0	-0.2	0.10	6.4
11.4	1.2	20.2	0.2	0.11	4.6
10.9	1.2	20.2	-0.1	0.11	4.0

IV. SPLASH ICING

We assume that splash drops are large enough that the collision efficiency is 1.

The seawater temperature is above freezing and the liquid water content at lower elevations in the splash plume is relatively high, so unless the air is cold, splash may not freeze on the structure and may even remove previously accreted splash ice. We assume that no ice accretes at elevations below $z = \chi + 0.5H_s$. Above this height, we use a simple heat balance algorithm, taking the salinity of the water into account by assuming a freezing temperature of -1.6°C, rounded up to compensate for ignoring any cooling of the splash plume. In the heat balance calculation, we consider convective and evaporative cooling and heat released by cooling the seawater to -1.6°C and by the latent heat of fusion. Depending on air temperature and humidity, wind speed, ocean temperature, and splash liquid water content, splash may accrete as ice or previously accreted ice may melt. The relatively fresh accreted ice (see section II) is also allowed to melt in periods without splash if the air temperature is above 0°C.

Splash icing on the leg of a wind turbine platform fixed to the bottom in 40-m deep water in the Baltic Sea is shown in Figure 7. Using the rung spacing for scale indicates a leg diameter of about 3 m. As access to the platform is by boat, the ice covering the ladder denied access. There is some weather and ocean data associated with that icing episode available (personal communication, Jacob Royle) but it has not been published. Mizuno et al [9] show splash icing on an experimental structure with 0.5-m diameter legs set on the bottom in the Sea of Japan in 7-m deep water. Weather and ocean data and photographs of the structure were collected from 1988 through at least 1990, but are no longer available (personal communication, Mitsunari Hirasawa).

Figure 7: Ice-covered leg of wind turbine platform in the Baltic Sea

V. Results and Discussion

The mast in WREx2 provides an example of splash icing, but with the splash generated by a rock face rather than by an engineered structure. The rock face is essentially vertical, but it bends over to horizontal near the top, and becomes jumbled large rocks where the point of land merges with the rest of the island. Depth of water at the rock face is about 5m. Weather and ocean data for WREx2 are shown in Figure 8. Air temperature and wind speed are measured from the lighthouse. Water temperature, significant wave height, and wavelength are measured at a buoy 15 km north. Note the 3 to 4 m tidal range. The bottom panel shows the modelled ice mass on the mast, assuming splash ice accreted with a uniform thickness and a density of 900 kg/m^3 on the windward half of the mast. The 6-day tick spacing on the horizontal axis matches the 6-day-long rows of photographs in Figure 4.

Splash data to fill in between values from the breakwater and the slender pile wave tank tests would better define the variation of both run-up and splash for the range of configurations of fixed offshore structures. It would also be useful to determine the effect of cross-sectional shape on splash. A field test in relatively deep water with structure widths of 5, 10, 25, 50, and 100 m, with both curved and flat sides would be ideal. Splash heights would be documented by high speed video, as in [6] and [7], with atmosphere and ocean measurements made from an instrumented buoy.

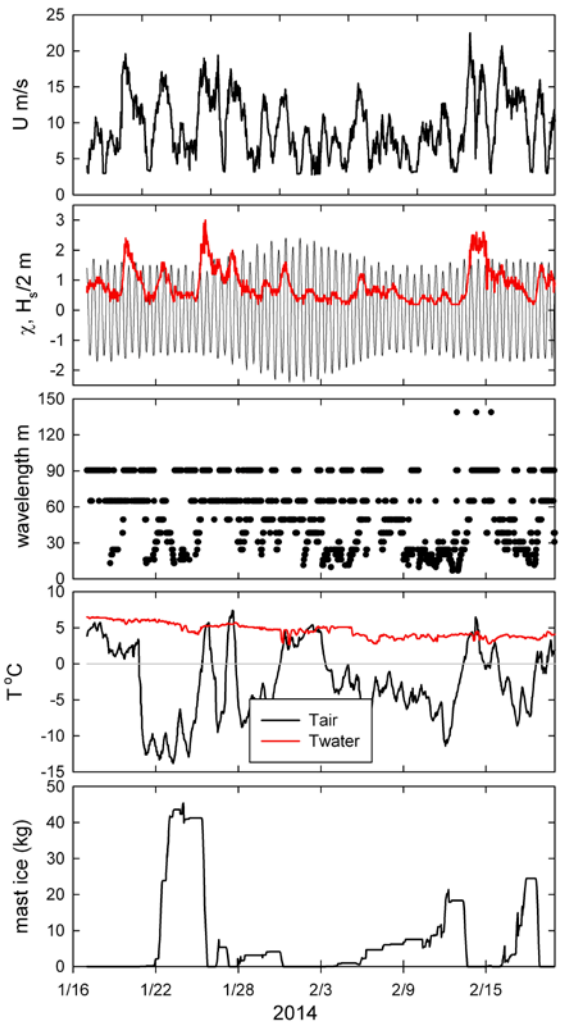

Figure 8. Mt. Desert Rock weather and ocean conditions and modelled ice mass on mast 17 Jan to 20 Feb 2014.

Acknowledgments

ONR Award Number N0001412MP20085 supported this work. We thank College of the Atlantic, Chris Tremblay, and Tanya Lubansky for providing logistics for WREx2.

References

[1] P. Mitten, Measurement and modeling os spray icing on offshore structures-Final report for Atmospheric Environment Service (1994) 70 pages.

[2] L. Horjen and S. Vensmo, Mobile platform stability (MOPS) subproject 02-icing, MOPS Report No. 15, Norwegian Hydrodynamic Laboratories, STF60 A 284002 (1984) 45 pages.

[3] T.W. Forest, E.P. Lozowski, R. Gagnon, Estimating marine icing on offshore structures using RIGICE04, *Proceedings of IWAIS XI* (2005).

[4] A. Kulyakhtin and A. Tsarau, A time-dependent model of marine icing with application of computational fluid dynamics, *Cold Regions Scince and Technology* **104-105** (2014) 33-44.

[5] L. De Vos, P. Frigaard, and J. De Rouck, Wave run-up on cylindrical and cones shaped foundations for offshore wind turbines, *Coastal Engineering* **54** (2007) 17-29.

[6] J. Ramirez, P. Frigaard, T. Lykke Andersen, L. De Vos, Large scale model test investigation on wave run-up in irregular waves at slender piles, *Coastal Engineering* **72** (2013) 69-79.

[7] M. Yamashire, A. Yoshida, Y. Nishi, Effects of wave dissipating blocks on reduction of salinity in the air generated at a vertical breakwater based on field observations, *Coastal Engineering Journal* **54**, 3 (2012) 1250019, 24 pages.

[8] T. Lykke Andersen, P. Frigaard, M.L. Damsgaard, L. DeVos, Wave run-up on slender piles in design conditions-Model tests and design rules for offshore wind, *Coastal Engineering* **58** (2011) 281-289.

[9] Y. Mizuno, M Hirasawa, K. Yano, K. Tokikawa (1991) Investigation of sea spray icing on offshore structure, *Proceedings of 1st International Offshore and Polar Engineering Conference* (1991) 543-547.